A Small-Angle X-ray Scattering Study of Complexes Formed in Mixtures of a Cationic Polyelectrolyte and an Anionic Surfactant

5 AUTHORS, INCLUDING:

Magnus Bergstrom

Uppsala University

62 PUBLICATIONS   1,566 CITATIONS

Jan Skov Pedersen

Aarhus University

363 PUBLICATIONS   10,961 CITATIONS

Martin Meedom Nielsen

Technical University of Denmark

112 PUBLICATIONS   6,632 CITATIONS

ARTICLES

A Small-Angle X-ray Scattering Study of Complexes Formed in Mixtures of a Cationic Polyelectrolyte and an Anionic Surfactant

Magnus Bergström,*,† U. R. Mikael Kjellin,† Per M. Claesson,† Jan Skov Pedersen,‡ and Martin M. Nielsen§

Department of Chemistry, Surface Chemistry, Royal Institute of Technology, Drottning Kristinas väg 51, SE-100 44 Stockholm, Sweden, and YKI, Institute for Surface Chemistry, Box 5607, SE-114 86 Stockholm, Sweden, Department of Chemistry, University of Aarhus, DK-8000 Aarhus C, Denmark, and Danish Polymer Center, Risø National Laboratory, DK-4000 Roskilde, Denmark

Received: April 18, 2002

The internal structure of the solid phase formed in mixtures of the anionic surfactant sodium dodecyl sulfate (SDS) and a range of oppositely charged polyelectrolytes with different side chains and charge density has been investigated using small-angle X-ray scattering. Polyelectrolytes with short side chains ([3-(2-methylpropionamido)propyl]trimethylammonium chloride, MAPTAC, and poly{[(2-propionyloxy)ethyl]-trimethylammonium chloride}, PCMA) form a 2-dimensional hexagonal structure with SDS, whereas a polyelectrolyte without side chains (poly(vinlyamine), PVAm) forms a lamellar structure. The hexagonal structure of MAPTAC is retained either when a neutral monomer (acrylamide, AM) is included in the polymer backbone to reduce the charge density or when a nonionic surfactant is admixed to the SDS/polyelctrolyte complex. The unit cell length of AM-MAPTAC increases with decreasing charge density from $a = 47.7$ Å (MAPTAC, 100% charge density) to 58.5 Å (AM-MAPTAC, 30% charge density). The unit cell length in the lamellar SDS/PVAm complex ($a = 36.1$ Å) is significantly smaller than for the different hexagonal structures. It is conjectured that the cylinders in the hexagonal structure and the bilayers in the lamellar structure are based on self-assembled surfactant aggregates with the polyelectrolyte mainly located in the aqueous region adjacent to the charged surfactant headgroups.

Introduction

The association between polyelectrolytes and oppositely charged surfactants has been extensively studied, both in bulk and at interfaces, and many recent reviews and books covering different aspects are available.[1–8] In particular, it is found that the association is mainly driven by hydrophobic interactions, mainly between the surfactant tails, as well as the entropic gain caused by the release of oppositely charged counterions. The reduction of the chemical potentials of aggregated surfactant and polyelectrolyte due to the release of counterions implies that the surfactant concentration at which the association occurs, the critical association concentration (cac), is lower than the corresponding critical micelle concentration (cmc) at which pure surfactants start to self-assemble.

The structure of charged surfactant/polymer complexes has been characterized with several techniques, and it is found to strongly depend on the system under investigation. For instance, Cosgrove et al.[9] studied complexes between gelatin (having both anionic and cationic sites) and sodium dodecyl sulfate (SDS) and concluded from SANS measurements that micelle-like

structures were formed along the polyelectrolyte chain in a bead-and-necklace structure, i.e., an arrangement similar to that for the well-characterized complexes formed between uncharged poly(ethylene oxide) and SDS.[10,11] On the other hand, Antonietti and co-workers[12–16] found by wide-angle X-ray (WAXS) studies that several polyelectrolyte–surfactant complexes formed ordered lamellar structures with a rather complex topology. Merta et al.[17] have studied a complex phase formed in mixtures of cationic starch and a range of anionic surfactants and observed ordered lamellar, 2-dimensional hexagonal, and various cubic structures depending on the surfactant tail or headgroup. Illekti et al.[18,19] investigated aqueous mixtures of the anionic polyelectrolyte sodium polyacrylate and the cationic surfactant cetyltrimethylammonium bromide (CTAB) and observed hexagonal as well as cubic structures, depending on surfactant and polyelectrolyte concentrations, to form in a complex phase. More recently, Svensson et al.[20] studied the related system of CTAB and the polyelectrolyte/surfactant complex cetyltrimethylammonium polyacrylate (CTAPA) in water. They observed a rather complex phase behavior where a diluted ([CTAPA] < 50 wt %) hexagonal as well as a cubic phase (50 wt % < [CTAPA] < 55 wt %) was observed as water was added to pure CTAPA.

We have recently investigated aqueous mixtures of the cationic polyelectrolyte poly{[(2-propionyloxy)ethyl]trimethylammonium chloride} (PCMA) (cf. Figure 1) and the (deu-

* Corresponding author. E-mail: magnus.bergstrom@surfchem.kth.se. Tel: +46 8 790 99 05. Fax: +46 8 20 89 98.
† Royal Institute of Technology and Institute for Surface Chemistry.
‡ University of Aarhus.
§ Risø National Laboratory.

SAXS of Complexes in SDS and Polyelectrolytes

J. Phys. Chem. B, Vol. 106, No. 44, 2002 **11413**

PCMA

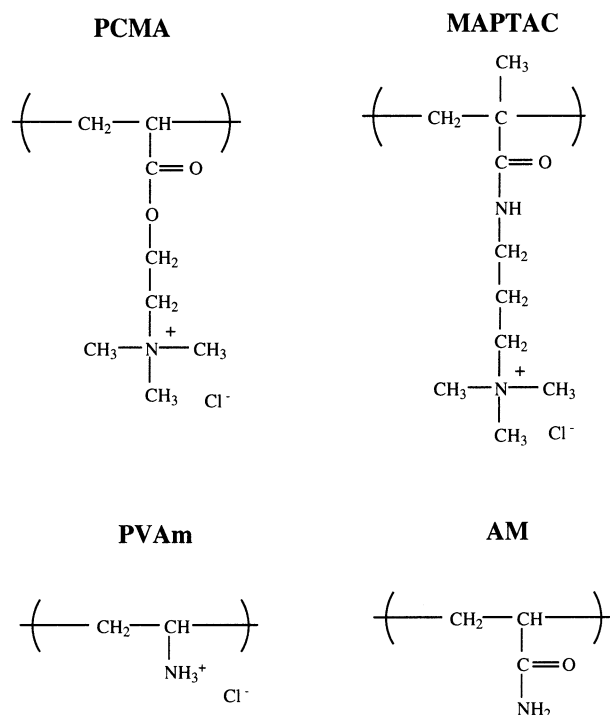**MAPTAC**

PVAm

AM

Figure 1. Chemical structures of [2-(propionlyoxy)ethyl]trimethylammonium chloride (CMA), [3-(2-methylpropionamido)propyl]trimethylammonium chloride (MAPTAC), acrylamide (AM), and vinylamine (VAm).

terated) anionic surfactant sodium dodecyl sulfate (d-SDS) with small-angle neutron scattering (SANS).[21] After mixing the samples, a phase separation into a white precipitate and a transparent water solution occurred for samples with a ratio $r \equiv$ [total charge of d-SDS]/[total charge of polyelectrolyte] = 0.25−1.5. We studied the samples in pure D$_2$O, where d-SDS is nearly contrast matched, as well as in a D$_2$O/H$_2$O mixture, which corresponds to the match point of polyelectrolyte. For both solvents a sharp but resolution-limited peak from the PCMA/d-SDS complex appears in the SANS spectra at a scattering vector $q = 0.165$ Å^{-1} corresponding to a repeat distance of 38 Å. The modulus of the scattering vector q is given by $q = 4\pi \sin \theta/\lambda$, where 2θ is the angle between the direct and scattered beam and λ is the neutron wavelength. At low q values the scattering intensity decays as $I \propto q^{-4}$ characteristic for a three-dimensional structure and consistent with the formation of a precipitate that may be observed with the bare eye.

Moreover, from the scattering behavior of the various samples we could conclude that free PCMA is present in the liquid phase at an excess amount of polyelectrolyte ($r < 1$), the concentration of which decreases as r approaches unity. Likewise, free SDS micelles are present at $r > 1$, the concentration of which increases with increasing r above unity. We could, however, not observe any additional structure coexisting with the one characteristic for the precipitate ($I \propto q^{-4}$ at low q values and a Bragg peak at $q = 0.165$ Å^{-1}) in charge-neutralized solutions ($r = 1$). These observations are consistent with the idea that the precipitate consists of a charged neutralized mixture of PCMA/d-SDS, whereas the aqueous phase contains excess (if any) polyelectrolyte or surfactant. As a consequence of a condition that the surfactant/polyelectrolyte complexes must be charge neutralized, a pair of small counterions (Na$^+$ and Cl$^-$ in the present study) must be released into the exterior aqueous bulk phase, where its entropy of mixing is much larger, as the

two oppositely charged components are self-assembled. This picture is also supported by SANS and small-angle X-ray scattering (SAXS) experiments on similar polyelectrolyte/SDS complexes to be discussed below in the present paper. We may, however, note that electrophoretic mobility measurements of dispersed polyelectrolyte/SDS complexes in dilute solutions in the presence of excess surfactant show that the particles contain an excess of the anionic surfactant.[22] This is most likely due to adsorption of an outer layer of surfactant that is charge compensated by a diffuse layer of small counterions. The interior of the particle is, however, expected to be uncharged. Consequently, a small amount of very small particles, for which the charge per volume may be nonnegligible, may be dissolved in the aqueous phase.

To investigate the structure of the complexes formed by SDS and cationic polyelectrolyte as a function of charge density of the polyelectrolyte, we have performed SANS and SAXS measurements of mixtures of SDS (or d-SDS) and AM-MAPTAC where the fraction of the monomers AM (acrylamide) and MAPTAC ([3-(2-methylpropionamido)propyl]trimethylammonium chloride) in the polyelectrolyte is set so as to give charge densities 10, 30, 60, and 100%. The SAXS data will be presented below, whereas the results from the SANS measurements will be given in a separate forthcoming publication. Nevertheless, we will below briefly discuss the most important conclusions that are drawn from the SANS measurements and are relevant for the interpretation of our SAXS data. In addition to (charge-neutralized) mixtures of SDS and polyelectrolytes from the AM-MAPTAC series, we have also investigated (charge-neutralized) mixtures of SDS on one side and PCMA, poly(vinylamine) (PVAm), and AM-MAPTAC30 (30% of the monomers (MAPTAC) of the polyelectrolyte carry one positive charge) together with a nonionic surfactant on the other side.

Materials and Methods

Materials. We have investigated charge-neutralized mixtures of a range of cationic polyelectrolytes and the anionic surfactant sodium dodecyl sulfate (SDS). The polyelectrolytes used in this study were poly{[3-(2-methylpropionamido)propyl]trimethylammonium chloride} (MAPTAC) with a number averaged molecular mass of 480 kg/mol or 2600 monomer segments per molecule, poly{[2-(propionlyoxy)ethyl]trimethylammonium chloride} (PCMA, 1600 kg/mol or 10 100 monomer segments per molecule), and poly(vinylamine) (PVAm, 90 kg/mol or 2000 monomer segments per molecule). Each monomeric segment of these polyelectrolytes carries one positive charge. We also used polyelectrolytes with a mixture of a charged monomer (MAPTAC) and the noncharged monomer acrylamide (AM) so as to give a charge density of 30% (AM-MAPTAC30, 780 kg/mol or 7400 monomer segments per molecule) and 60% (AM-MAPTAC60, 340 kg/mol or 2400 monomer segments per molecule). The quaternary ammonium cationic groups on the AM-MAPTAC and PCMA are located on short side chains, whereas the polyelectrolyte backbone is linear. In contrast, the charged groups on PVAm are primary amines located next to the polymer backbone. The structural elements for all polyelectrolytes are shown in Figure 1. PCMA, MAPTAC, AM-MAPTAC30, and AM-MAPTAC60 were synthesized and kindly provided by the Laboratoire de Physico-Chimie Macromoleculaire, Université Pierre et Marie Curie, Paris. PVAm was obtained from BASF AG, Ludwigshafen, Germany, as a 12% aqueous solution and was purified by recrystalization.[23] PVAm was titrated with HCl to reach pH 7 where it is 100% charged.

In addition we have investigated charge-neutralized mixtures of 30% charged AM-MAPTAC and SDS with the three different
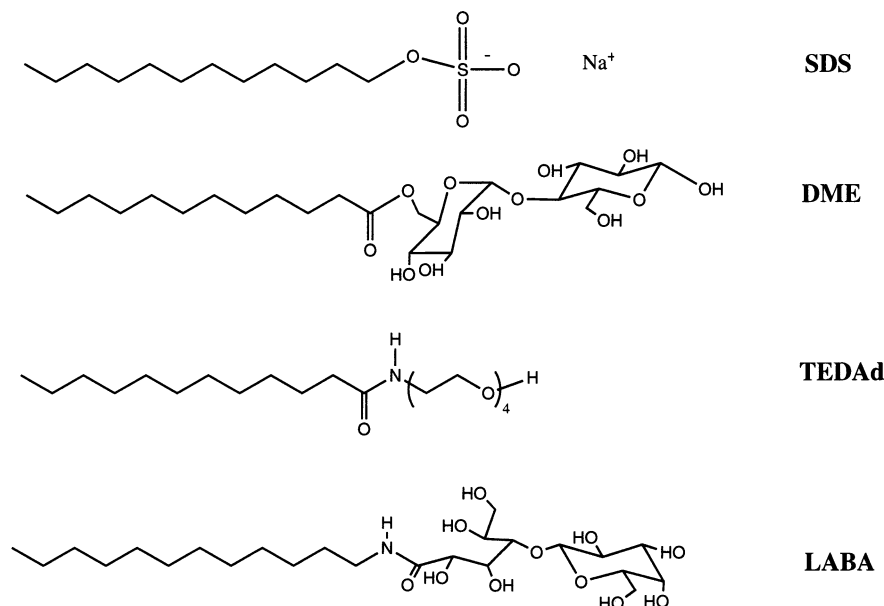
Figure 2. Chemical structures of sodium dodecyl sulfate (SDS), maltose 6′-O-dodecanoate (DME), tetra(ethylene oxide)dodecylamide (TEDAd), and *N*-dodecyllactobionamide (LABA).

nonionic surfactants: maltose 6′-O-dodecanoate (DME), tetra-(ethylene oxide)dodecylamide (TEDAd), and *N*-dodecyllacto-bionamide (LABA) where the molar ratio of ionic/nonionic surfactant was 1:2 for all samples. SDS (>99% purity) was obtained from BDH and used without further purification. TEDAd (>99% purity) and LABA (> 95% purity) were synthesized and purified by Akzo Nobel Surface Chemistry in Stenungsund, Sweden. DME was kindly provided from Professor Evgeny N. Vulfson, Department of Macromolecular Science, Institute of Food Research, Reading, U.K.. The structures of the surfactants are shown in Figure 2.

The samples were prepared by simply mixing polyelectrolye and surfactant so as to yield a concentration of polyelectrolyte equal to 1 wt % and a concentration of surfactant corresponding to charge neutralization ([SDS] = 1.3 wt % for MAPTAC, 1.2 wt % for AM-MAPTAC60, 0.75 wt % for AM-MAPTAC30, 1.5 wt % for PCMA and 6.5 wt % for PVA). In all mixtures we have studied, a white precipitate was formed together with an isotropic aqueous phase. The precipitate was concentrated and transferred to the sample cell together with a small amount of excess liquid phase. Hence, we have not dried the solid phase since it might influence its internal structure. This means that small particles from the solid phase might be dispersed in the aqueous phase and, therefore, it is difficult to completely separate the two phases from each other.

Methods. The structures of the precipitates were investigated by SAXS. The instrument at Risø National Laboratory, Roskilde, Denmark, was applied. The source is an 18 kW Rigaku Ru H3R rotating anode with a Cu target. The anode is usually operated at 15 kW to ensure stable operating conditions. The beam is monochromatized by a graphite crystal and collimated by three sets of square slits, of which the two first define the beam and the last one acts as a guard slit cutting away parasitic scattering. The scattered X-rays are recorded with a two-dimensional position-sensitive proportional counter. A beamstop is located in front of the detector to prevent damage by the direct intense beam. The instrument covers a range $0.01-0.5$ Å^{-1} for the modulus of the scattering vector q. The collimation length is about 120 cm, and the sample to detector distance is about 110 cm. The instrument is equipped with an automatic sample changer, which can take 10 samples at the same time. The samples were kept in borosilicate glass capillary tubes with a diameter of 2 mm. The samples are located in air and two Kapton windows separate the sample area from the rest of the instrument, which is evacuated to reduce the background. The white precipitate material was transferred to the glass capillaries using a syringe. A capillary with pure water was also measured as a background. The two-dimensional spectra were azimuthally averaged and thus reduced to intensity versus scattering vector q. The transmission of the samples and the water was determined from measurements on a strongly scattering glassy carbon sample with and without the samples inserted in the beam. The background was scaled with the relative transmission of samples and water and subtracted. The wavelength resolution of the SAXS camera is about 1% compared to 9% for the previously used SANS instrument. This makes the SAXS camera much better suited for locating higher order reflections. The Kapton windows gives rise to a broad peak at around $q = 0.4$ Å^{-1}, which sometimes prevents the observation of peaks from the samples in this region.

Crystallographic Interpretation of SAXS Data

The regular pattern in a crystal gives rise to a sequence of Bragg-like peaks in the scattering data, the relative locations of which depend on the repeat unit of the crystal. The peaks in the scattering spectra are the results of interplanar spacings d_{hkl} in the crystal, where h, k, and l are integer numbers denoted by the Miller indices, so that the peak positions are located at $q_{hkl} = 2\pi/d_{hkl}$. For a structure that is periodic in only one dimension, e.g., stacks of lamellar sheets ordered on top of each other, $k = l = 0$ and in the corresponding scattering spectra a series of peaks appear located at $q_h = 2\pi/d_h = 2\pi h/a$, where a is the unit cell length. For this particular case a is equal to the distance between the centers of two lamellae and $h = 1, 2, 3$, etc. Similarly, for a two-dimensional hexagonal pattern of long rods $l = 0$ and

$$d_{hk} = \left[\frac{4}{3a^2}(h^2 + k^2 + hk)\right]^{-1/2} \tag{1}$$

SAXS of Complexes in SDS and Polyelectrolytes

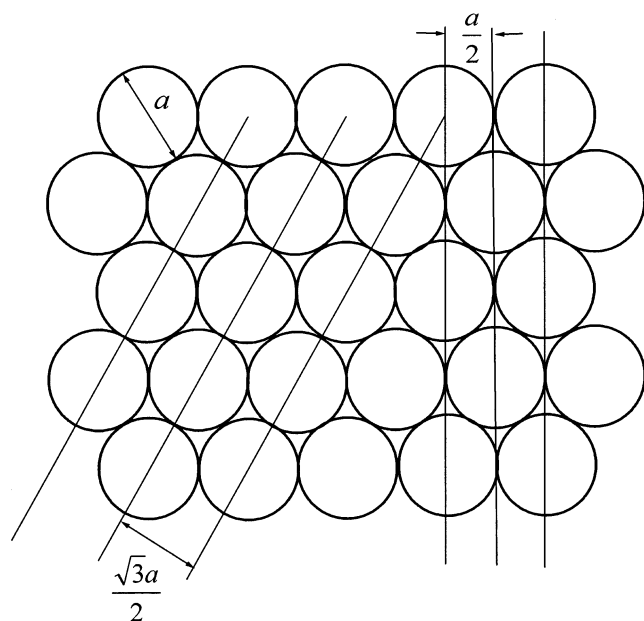*J. Phys. Chem. B, Vol. 106, No. 44, 2002* **11415**

Figure 3. Schematic representation of a hexagonal lattice of close packed cylinders with diameter a.

implying the peak positions in a SAXS spectrum to be located at

$$q_{hk} = \frac{2\pi}{d_{hk}} = \frac{4\pi}{\sqrt{3}a}\sqrt{h^2 + k^2 + hk} \qquad (2)$$

where the unit cell length a is the distance between the centers of two adjacent rods (cf. Figure 3). This means that the relative distance between Bragg peaks in a two-dimensional (2D) hexagonal structure is $q_{10}:q_{11}:q_{20}:q_{21}:q_{30}:q_{22} = 1:\sqrt{3}:2:\sqrt{7}:3:2\sqrt{3}$, etc.

The width of the peaks is inversely proportional to the correlation length of the ordered units, so that long-range correlations give sharp peaks and short-range correlations give broad peaks. The intensity of the peaks (i.e., the integrated area) is given by the distribution of scattering length density within the repeat unit. If there is only one scattering object within the unit cell, the intensity is proportional to the form factor of the objects. For the lamellar structure the object is obviously the lamella, and as the order extends in only one dimension, the intensity is proportional to the cross-section form factor of a lamella. For hexagonally ordered cylinders, the order extends in two dimensions, and the intensity is proportional to the cross-section form factor of the cylinders. Nonordered or "unbound" scattering objects will contribute with a structured background in the spectra.[24] The intensity of the structured background is also proportional to the form factor of the scattering objects.

Results and Discussion

Just by observing the samples we could see a precipitate at all [SDS]/[polyelectrolyte] ratios for the SDS/MAPTAC case and close to charge neutralization for the SDS/AM-MAPTAC30 and SDS/AM-MAPTAC60 cases ($0.6 < r < 1.2$) whereas the solutions appear transparent in sufficient excess of SDS or AM-MAPTAC30/AM-MAPTAC60 (cf. Figure 4). One sharp Bragg peak was seen in the SANS data of all samples containing precipitate similar to what was found for PCMA/d-SDS complexes.[21] The location of the peak is shifted toward lower q (i.e., larger interplanar spacing) with decreasing polyelectrolyte charge density. For the SDS/AM-MAPTAC10 case a white
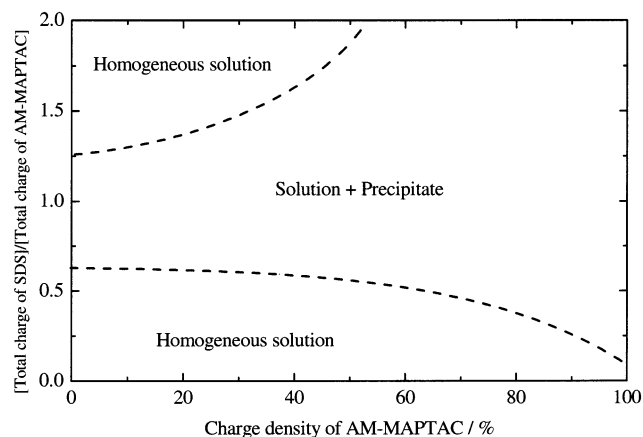

Figure 4. Diagram showing the different phases formed in mixtures of SDS and AM-MAPTAC with different charge densities. The surfactant/polyelectrolyte composition on the *y*-axis is expressed as $r \equiv$ [total charge of d-SDS]/[total charge of polyelectrolyte]. The total concentration of polyelectrolyte is always 1 wt %.

sticky gellike structure formed close to charge neutralization and in the corresponding SANS data a rather broad peak was seen at high q values ($q \approx 0.1$ Å^{-1}). Analogous to the PCMA/SDS case, free polyelectrolyte was seen to be present in the liquid phase at $r < 1$ and free SDS micelles at $r > 1$ for all samples where a precipitate forms (cf. Figure 4).

To evaluate the detailed structure of the precipitate, we have further investigated it with SAXS. For all samples one or more Bragg peaks were observed in the SAXS spectra at $q > 0.1$ Å^{-1}, the positions of which are given in Table 1. Expected peaks that could not readily be observed in the SAXS spectra are set within brackets. The location of the first peak for each sample is identical in the SANS and SAXS spectra.

In Table 1 we have also included the volume fractions of surfactant, polyelectrolyte and water in a unit cell as calculated from the appropriate molecular volumes[25] (88.3 Å^3 (AM), 293.1 Å^3 (MAPTAC), 237.7 Å^3 (CMA), 65.3 Å^3 (PVAm), 425.6 Å^3 (SDS), 674 Å^3 (DME), 630 Å^3 (TEDAd), and 700 Å^3 (LABA)). The concentration of surfactant was assumed to correspond to a radius of the hydrocarbon part of cylindrical "micelles" (excluding any polyelectrolyte) equal to 14 Å, and a bilayer thickness of 22 Å (the PVAm case), in accordance with model calculations of SDS cylindrical micelles[26] and bilayers.[27,28] These are somewhat smaller values than what corresponds to a fully stretched C_{12} chain ($=16.7$ Å) mainly as a result of hydrocarbon chain conformational entropy.[29] We may note that the fraction of water decreases with increasing magnitude of assumed radial distance.

Mixtures of AM-MAPTAC with Different Charge Densities and SDS. SAXS data for mixtures of SDS with MAPTAC, AM-MAPTAC60, and AM-MAPTAC30, respectively, are given in Figures 5−7. Four peaks could readily be observed for the precipitate formed by MAPTAC (Figure 5) as well as of AM-MAPTAC60 (Figure 6), whereas three clear peaks and one vague could be identified in the spectra of the SDS/AM-MAPTAC30 complex (Figure 7). The peak positions are located as $4\pi/\sqrt{3}a$, $4\pi/a$, $8\pi/\sqrt{3}a$, and $4\pi\sqrt{7}/\sqrt{3}a$, consistent with a 2D hexagonal structure (cf. Figure 3). The unit cell length a increases with decreasing charge density from $a = 47.7$ Å for MAPTAC to $a = 52.6$ Å for AM-MAPTAC60 and $a = 58.5$ Å for AM-MAPTAC30. This trend is suggested to be due to the fact that an increasing volume of noncharged polyelectrolyte segments must be incorporated into the surfactant/polyelectrolyte complex. In other words, the volume per charge of the

TABLE 1: Positions of Peaks Observed in SAXS Spectra of Precipitates Formed in Mixtures of Surfactant and Polyelectrolyte[a]

	peak I/Å^{-1}	peak II/Å^{-1}	peak III/Å^{-1}	peak IV/Å^{-1}	a/Å	ϕ_{surf}	ϕ_{pol}	ϕ_{wat}
AM-MAPTAC/SDS 1:1	0.152	0.265	0.304	0.405	47.7	0.38	0.26	0.36
AM-MAPTAC60/SDS 1:1	0.138	0.240	0.277	0.369	52.6	0.31	0.26	0.43
AM-MAPTAC30/SDS 1:1	0.124	0.214	0.247	(0.328)	58.5	0.25	0.30	0.45
PCMA/SDS 1:1	0.164	0.286	0.331	0.436	44.2	0.44	0.25	0.31
PVAm/SDS 1:1	0.174	0.349	(0.522)		36.1	0.74	0.11	0.15
AM-MAPTAC30/SDS/DME 1:1:2	0.129	0.225	0.260	(0.342)	56.2	0.40	0.11	0.49
AM-MAPTAC30/SDS/TEDAd 1:1:2	0.121	0.212	0.243	(0.320)	60.0	0.33	0.10	0.57
AM-MAPTAC30/SDS/LABA 1:1:2	0.121	0.212	0.243	(0.320)	60.0	0.34	0.09	0.56

[a] The sequence of peaks is consistent with a 2D hexagonal structure ($1/\sqrt{3}a$:$1/a$:$2/\sqrt{3}a$:$\sqrt{7}/\sqrt{3}a$) for all samples except PVAm/SDS, which is consistent with a 1D lamellar structure ($1/a$:$2/a$:$3/a$). The expected locations of peaks that are not clearly seen in the spectra are put within parentheses. The unit cell length a (cf. Figure 13) is also given as well as the volume fractions of surfactant (ϕ_{surf}), polyelectrolyte (ϕ_{pol}), and water (ϕ_{wat}) in a unit cell as calculated from the appropriate molecular volumes.
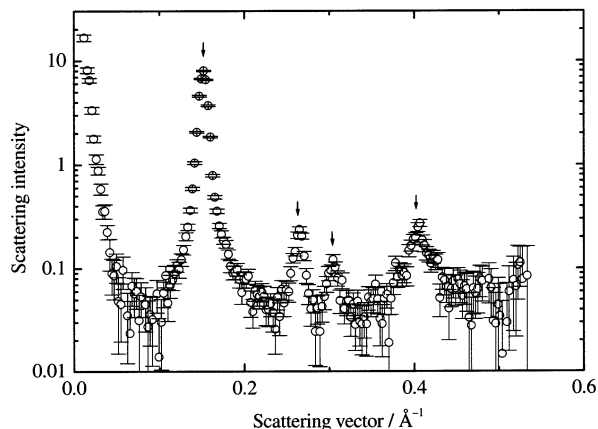
Figure 5. Small-angle X-ray scattering intensity as a function of scattering vector q for a charge-neutralized mixture of SDS and MAPTAC (100% charge density). The locations of the Bragg-like peaks are indicated with arrows.
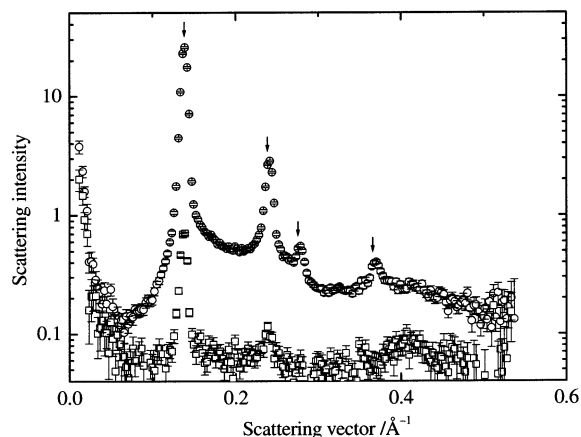
Figure 6. Small-angle X-ray scattering intensity as a function of scattering vector q for a charge-neutralized mixture of SDS and AM-MAPTAC60 (60% charge density). Circles refer to a sample where the precipitate has been concentrated by means of removing most of the aqueous solution, whereas squares refer to a mixture where precipitate coexists with a large excess of aqueous phase. The locations of the Bragg-like peaks are indicated with arrows.

polyelectrolyte increases with decreasing charge density. In accordance, it is seen in Table 1 that the fraction of surfactant is dramatically decreased with decreasing polyelectrolyte charge density. However, there is no clear trend in the ϕ_{pol}/ϕ_{wat} ratio, showing that an increasing amount of water also must be included in the crystals as the charge density decreases. The concomitant inclusion of polymer and water is favored by the entropy of mixing uncharged polymer segments and water.
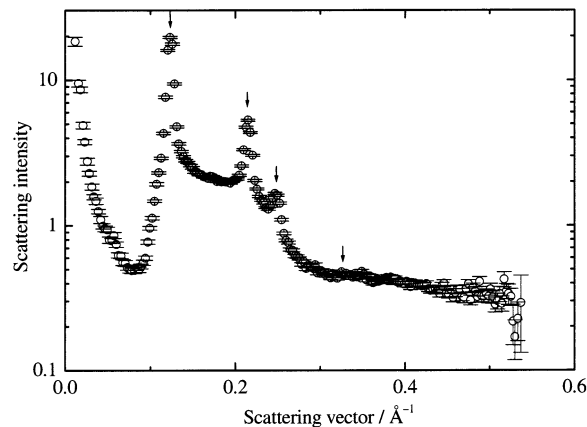
Figure 7. Small-angle X-ray scattering intensity as a function of scattering vector q for a charge-neutralized mixture of SDS and AM-MAPTAC30 (30% charge density). The locations of the Bragg-like peaks are indicated with arrows. The arrow at the highest q value indicates where the fourth peak of a 2D hexagonal structure is expected to be located.

For the fully charged polyelectrolyte there is no background from uncorrelated objects; however, the peaks are quite broad, corresponding to a relatively short range of the hexagonal correlations. The background originating from uncorrelated scattering objects increases as the charge density of the polyelectrolyte is decreased, showing that the amount of uncorrelated objects increases with an increasing volume of uncharged polymer segments and an increasing distance between two adjacent cylinders. The uncorrelated objects may consist of free cylinders dispersed in the excess of liquid phase present in the sample. On the other hand the peaks are narrow for the MAPTAC60 and MAPTAC30 samples, indicating a long range of the correlations within the ordered regions.

As for the SANS data, we could not observe small-angle X-ray scattering behavior consistent with free polyelectrolyte or SDS micelles in any of the charge-neutralized samples. Moreover, in Figure 6 we have also included the SAXS spectra of a sample with precipitate together with a substantial amount of aqueous phase. The two spectra only differ insofar as the intensity is much lower in the latter case because the amount of complex, which is mainly located in the precipitate, is lower. In other words, since no additional structure can be observed when the amount of the aqueous phase in the sample is increased, we may conclude that both surfactant and polyelectrolyte are incorporated into the solid phase, which, thus, may not contain any sodium or chloride counterions.

Mixtures of PCMA and SDS. SAXS data for mixtures of SDS and PCMA are given in Figure 8. Four peaks are readily identified, the positions of which are located as $4\pi/\sqrt{3}a$, $4\pi/a$,
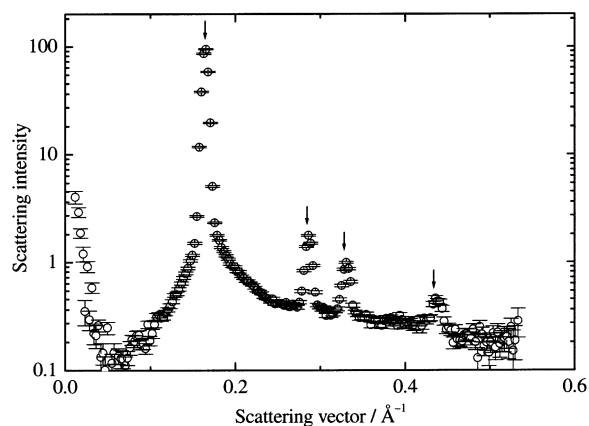
SAXS of Complexes in SDS and Polyelectrolytes

J. Phys. Chem. B, Vol. 106, No. 44, 2002 **11417**

Figure 8. Small-angle X-ray scattering intensity as a function of scattering vector q for a charge-neutralized mixture of SDS and PCMA (100% charge density). The locations of the Bragg-like peaks are indicated with arrows.
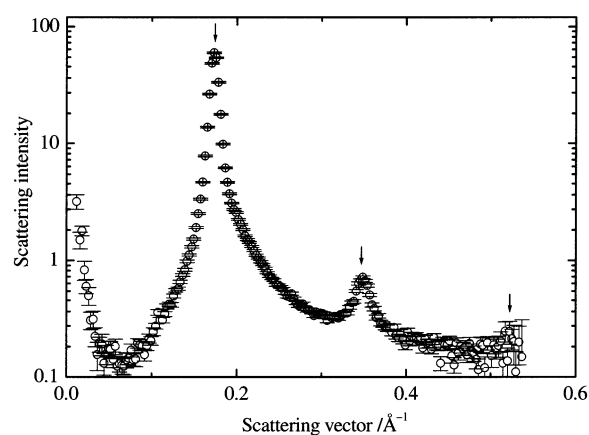

Figure 9. Small-angle X-ray scattering intensity as a function of scattering vector q for a charge-neutralized mixture of SDS and PVAm (100% charge density). The locations of the Bragg-like peaks are indicated with arrows. The arrow at the highest q value indicates where the third peak of a 1D lamellar structure is expected to be located.

$8\pi/\sqrt{3}a$, and $4\pi\sqrt{7}/\sqrt{3}a$, consistent with a 2D hexagonal structure. The unit cell length $a = 44.2$ Å, which is somewhat less than the corresponding value for 100% charged MAPTAC ($a = 47.7$ Å). This is consistent with the somewhat shorter side chains of PCMA as compared with MAPTAC; i.e., the volume per charge is lower for PCMA. Note that the unit cell length is larger than the interlayer spacing (=38 Å), which is the distance measured with SANS described in the Introduction and given in ref 21. The amount of structured background appears larger than for the MAPTAC case but is significantly less than for the complexes formed by AM-MAPTAC30 and AM-MAP-TAC60. We have no explanation for the difference between PCMA and MAPTAC with this respect. The peaks are narrow, which shows that there is long range order in the ordered regions.

Mixtures of PVAm and SDS. SAXS data for mixtures of SDS and PVAm are given in Figure 9. Two peaks are readily observed located at $2\pi/a$ and $4\pi/a$ with $a = 36.1$ Å. This is consistent with a one-dimensional lamellar structure but not with a 2D hexagonal structure, as were the cases for MAPTAC and PCMA. The peaks are broader than the instrumental resolution of the SAXS instrument, and thus the order has a finite range. The structured background suggests that uncorrelated objects, possibly free lamellar disks in the excess liquid phase, are also present.
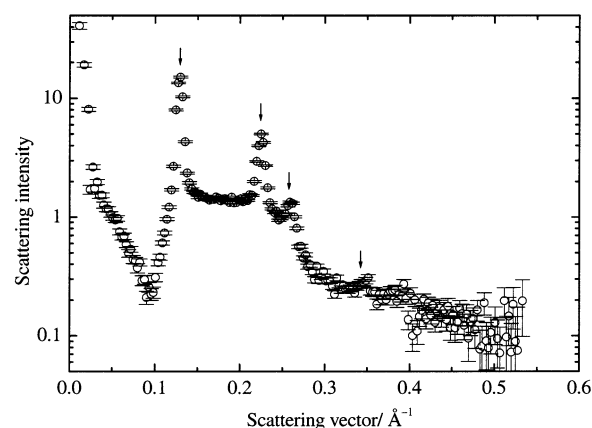

Figure 10. Small-angle X-ray scattering intensity as a function of scattering vector q for a charge-neutralized mixture of SDS, AM-MAPTAC30 (30% charge density), and DME. The molar ratio between SDS and DME is 1:2. The locations of the Bragg-like peaks are indicated with arrows.
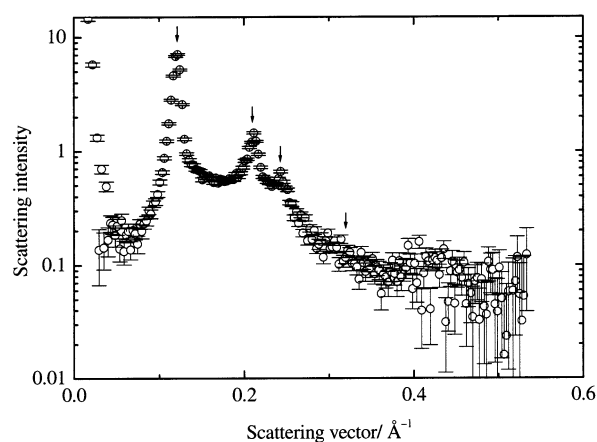

Figure 11. Small-angle X-ray scattering intensity as a function of scattering vector q for a charge-neutralized mixture of SDS, AM-MAPTAC30 (30% charge density), and TEDAd. The molar ratio between SDS and TEDAd is 1:2. The locations of the Bragg-like peaks are indicated with arrows. The arrow at the highest q value indicates where the fourth peak of a 2D hexagonal structure is expected to be located.

Mixtures of AM-MAPTAC30, SDS and a Nonionic Surfactant. The precipitate formed in charge-neutralized mixtures of AM-MAPTAC30, SDS, and the nonionic surfactants DME, TEDAd, and LABA (cf. Figure 2) was investigated, and the corresponding SAXS data are given in Figures 10−12, respectively. The molar ratio between SDS and nonionic surfactant was 1:2. Three peaks could readily be seen in each spectra, all of them located as $4\pi/\sqrt{3}a$, $4\pi/a$, $8\pi/\sqrt{3}a$, as well as the indication of a fourth peak at $4\pi\sqrt{7}/\sqrt{3}a$. This is again consistent with a 2D hexagonal structure. The unit cell length for the sample containing DME is slightly less ($a = 56.2$ Å) than for the AM-MAPTAC30/SDS mixture ($a = 58.5$ Å), whereas the corresponding quantity for mixtures containing TEDAd and LABA is somewhat larger ($a = 60$ Å for both mixtures) than for AM-MAPTAC30/SDS.

For all three samples, the peaks are narrow and the order is thus long range. There is also a significant amount of structured background, presumably due to the presence of uncorrelated cylinders in the excess liquid phase.

As for the previous samples, the scattering behavior is not consistent with the presence of free polyelectrolyte or surfactant micelles. Hence, we may conclude that, apart from some small
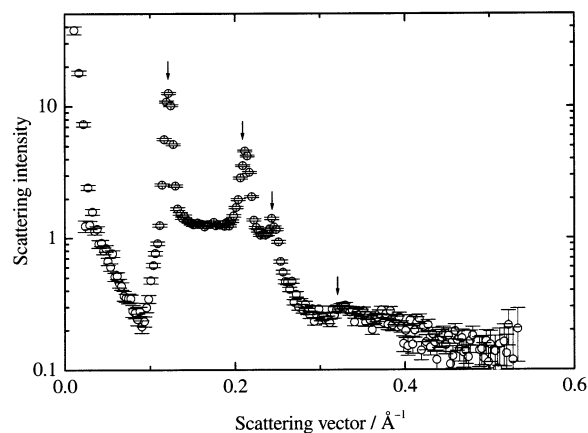
Figure 12. Small-angle X-ray scattering intensity as a function of scattering vector q for a charge-neutralized mixture of SDS, AM-MAPTAC30 (30% charge density), and LABA. The molar ratio between SDS and LABA is 1:2. The locations of the Bragg-like peaks are indicated with arrows. The arrow at the highest q value indicates where the fourth peak of a 2D hexagonal structure is expected to be located.
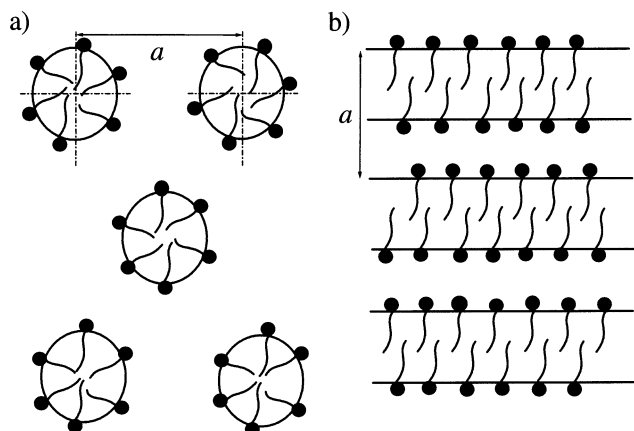

Figure 13. Schematic representations of (a) 2D hexagonal structure of cylindrical surfactant micelles and (b) 1D lamellar structure of surfactant bilayers with an aqueous region separating the hydrophobic cores. The polyelectrolyte must either be located in the aqueous region or, possibly, be partitioned between the hydrophobic and hydrophilic regions.

amount of free surfactant ($\approx$cmc), the nonionic surfactant is incorporated into the surfactant/polyelectrolyte complexes.

Structure of Polyelectrolyte/Surfactant Complexes. Schematic representations of the two lattice structures consistent with SAXS data are given in Figure 13. For all but one case the complexes formed are ordered in a 2D hexagonal pattern (Figure 13a). The exception is the precipitate formed by the nonbranched polyelectrolyte PVAm mixed with SDS where the scattering behavior is consistent with a 1D lamellar structure (Figure 13b). As already discussed, the hexagonal structure is due to the ordering of rods or cylinders. It is reasonable to assume that in our cases, the surfactant aggregates and forms cylinders or bilayers (PVAm/SDS mixture) with the hydrocarbon moieties forming the interior core and the headgroups located at the surface. The opposite charges of the polyelectrolyte must be located adjacent to the negative charges of the surfactant headgroups at the cylinder/bilayer surface. Of the samples given in Table 1 forming a hexagonal structure, the lowest value of the unit cell length is obtained for the PCMA/SDS mixture equalling $a = 44$ Å. The cross-section radius of the hydrocarbon part of cylindrical SDS micelles has been calculated to 14 Å

from a detailed model.[26] This would give a distance of about 16 Å between two adjacent cylinders where surfactant head-groups, polyelectrolyte, and water molecules are expected to be residing. As the polyelectrolyte charge density decreases, i.e., as the volume per charge of the polyelectrolyte increases, more material (polymer + water) must be gathered together with the surfactants and, as a result, the unit cell length increases. In a lamellar structure the aggregates may be packed more densely entirely because of geometrical reasons and, hence, the fraction of surfactant is much larger for the PVAm/SDS complexes ($\phi_{\text{surf}} = 0.74$ for PVAm and $\phi_{\text{surf}} = 0.44$ for PCMA, cf. Table 1). This tendency is enhanced by the smaller value of the unit cell length ($a = 36$ Å) in the latter case.

In most cases, long range order is present in the ordered regions. The exception is the fully charged MAPTAC with SDS and PVAm/SDS. All samples, except MAPTAC/SDS, display a spectrum with a structured background from uncorrelated scattering objects. The structure of the background is similar for all AM-MAPTAC samples, which shows that the cylinders formed by the surfactants have a similar structure. However, the correlated background observed for the complexes formed by 100% charged PCMA and PVAm is not insignificant, although it appears to be less than for the samples prepared by lower charged AM-MAPTAC. It should finally be noticed that the intensity of the Bragg-like peaks is proportional to the intensity of the structured background, as it should be when the intensity is the result of the product of a form factor for the uncorrelated scattering objects and a structure factor for the ordering.

Conclusion

We have investigated the internal structure of the solid phase formed in mixtures of an anionic surfactant (SDS) and cationic polyelectrolytes with different side chains and charge densities using small-angle X-ray scattering. Complexes formed by 100% charged polyelectrolytes with short side chains (PCMA and MAPTAC) form a 2D hexagonal structure that may be identified from the SAXS spectra by three Bragg-like peaks located as $4\pi/\sqrt{3}a$, $4\pi/a$, and $8\pi/\sqrt{3}a$, where a is the unit cell length. The hexagonal structure is retained when the charge density of MAPTAC is reduced by incorporation of neutral AM segments in the polyelectrolyte chains and the unit cell length increases with decreasing charge density or, otherwise expressed, increasing volume per charge of the polyelectrolyte. On the other hand, a cationic polyelectrolyte with no side chains (PVAm) forms a lamellar structure with SDS identified by the Bragg-like peak sequence $2\pi/a$ and $4\pi/a$ and the unit cell length is found to be considerably smaller ($a = 36.1$ Å) than for the corresponding hexagonal structures formed by MAPTAC ($a = 47.7$ Å) and PCMA ($a = 44.2$ Å). The larger unit cell length of SDS/MAPTAC complexes, as compared with the corresponding PCMA complexes, may be explained by the longer side chain of MAPTAC. Admixing a nonionic surfactant to a charge-neutralized mixture of SDS and AM-MAPTAC30 does not change the hexagonal structure of the complex. The unit cell length might increase (TEDAd and LABA) or decrease (DME) depending on the structure of the nonionic surfactant. It is conjectured that the ordered cylinders in the hexagonal structure or the bilayers in the lamellar structure of the complexes are based on self-assembled surfactants with polyelectrolye either located in the aqueous region adjacent to the charged surfactant headgroups or partitioned between the hydrophobic (surfactant tails) and the hydrophilic (surfactant headgroups and water) regions of the complexes.

References and Notes

(1) Wei, Y.-C.; Hudson, S. M. *J. Macromol. Sci., Rev. Macromol. Chem. Phys.* **1995**, *C35*, 15.

(2) LI, Y.;.L., D. P. In *Structure and Flow in Surfactant Solutions*; Herb, C. A., Prud'homme, R. K., Eds.; American Chemical Society: Washington, DC, 1994; Vol. 578, p 320.

(3) Goddard, E. D.; Ananthapadmanabhan, K. P. *Interactions of Surfactants with Polymers and Proteins*; CRC Press: Boca Raton, FL, 1993.

(4) Kwak, J. C. T. *Polymer-Surfactant Systems*; Marcel Dekker, Inc.: New York, 1998; Vol. 77.

(5) Piculell, L.; Lindman, B. *Adv. Colloid Interface Sci.* **1992**, *41*, 149.

(6) Piculell, L.; Guilemet, F.; Thuresson, K.; Shubin, V.; Ericsson, O. *Adv. Colloid Interface Sci.* **1996**, *63*, 1.

(7) Iliopoulos, I. *Curr. Opin. Colloid Interface Sci.* **1998**, *3*, 493.

(8) Claesson, P. M.; Dedinaite, A.; Poptoshev, E. *Physical Chemistry of Polyelectrolytes*; Marcel Dekker: New York, 2001; Vol. 99; p 447.

(9) Cosgrove, T.; White, S. J.; Zarbakhsh, A.; Heenan, R. K.; Howe, A. M. *Langmuir* **1995**, *11*, 744.

(10) Cabane, B.; Duplessix, R. *J. Phys. Fr.* **1982**, *43*, 1529.

(11) Cabane, B.; Duplessix, R. *Colloid Surf.* **1985**, *13*, 19.

(12) Antonietti, M.; Conrad, J.; Thünemann, A. *Macromolecules* **1994**, *27*, 6007.

(13) Antonietti, M.; Kaul, A.; Thünemann, A. *Langmuir* **1995**, *11*, 2633.

(14) Antonietti, M.; Burger, C.; Effing, J. *Adv. Mater.* **1995**, *7*, 751.

(15) Antonietti, M.; Wenzel, A.; Thünemann, A. *Langmuir* **1996**, *12*, 2111.

(16) Antonietti, M.; Maskos, M. **1996**, *29*, 4199.

(17) Merta, J.; Torkkeli, M.; Ikonen, T.; Serimaa, R.; Stenius, P. *Macromolecules* **2001**, *34*, 2937.

(18) Ilekti, P.; Piculell, L.; Tournilhac, F.; Cabane, B. *J. Phys. Chem. B* **1998**, *102*, 344.

(19) Ilekti, P.; Martin, T.; Cabane, B.; Piculell, L. *J. Phys. Chem. B* **1999**, *103*, 9831.

(20) Svensson, A.; Piculell, L.; Cabane, B.; Ilekti, P. *J. Phys. Chem. B* **2002**, *106*, 1013.

(21) Claesson, P. M.; Bergström, M.; Dedinaite, A.; Kjellin, M.; Legrand, J. F.; Grillo, I. *J. Phys. Chem. B* **2000**, *104*, 11689.

(22) Dedinaite, A.; Claesson, P. M. *Langmuir* **2000**, *16*, 1951.

(23) Poptoshev, E.; Rutland, M. W.; Claesson, P. M. *Langmuir* **1999**, *15*, 7789.

(24) Pabst, G.; Rappolt, M.; Amenitsch, H.; Laggner, P. *Phys. Rev. E* **2000**, *62*, 4000.

(25) Cabani, S.; Gianni, P.; Mollica, V.; Lepori, L. *J. Solution Chem.* **1981**, *10*, 563.

(26) Eriksson, J. C.; Ljunggren, S. *J. Chem. Soc., Faraday Trans. 2* **1985**, *81*, 1209.

(27) Ljunggren, S.; Eriksson, J. C. *J. Chem. Soc., Faraday Trans. 2* **1986**, *82*, 913.

(28) Bergström, M.; Eriksson, J. C. *Langmuir* **1996**, *12*, 624.

(29) Gruen, D. W. R. *J. Phys. Chem.* **1985**, *89*, 146.